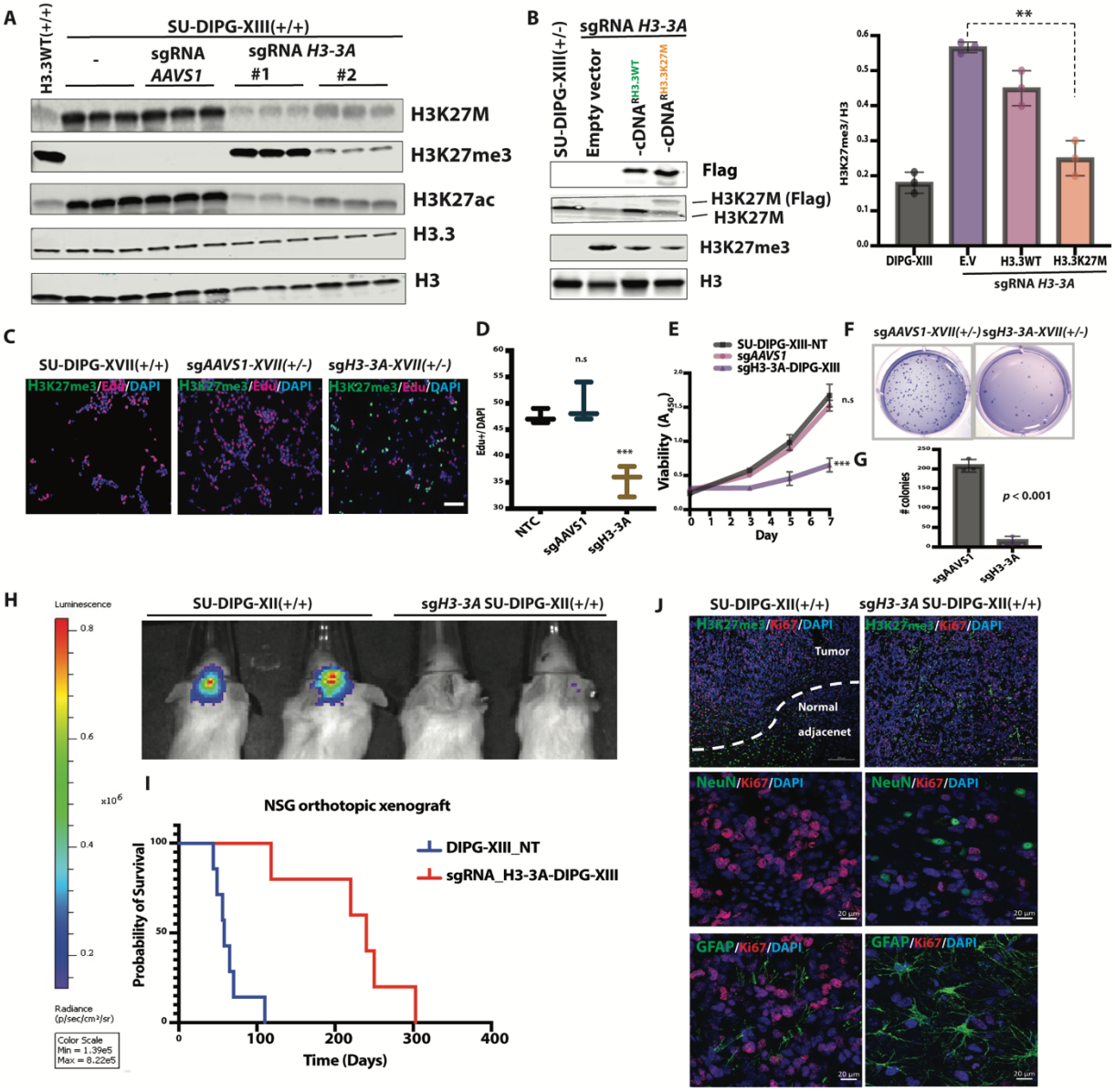

Fig. S1. CRISPR-Cas9 depletion of H3.3K27M rescued H3K27 trimethylation and delayed growth of patient-derived neurospheres and orthotopic xenografts. (A) Immunoblots assessing H3.3K27M CRISPR-knockout efficiency and epigenetic changes in DIPG patient cells; **(B)** Representative immunoblots of H3.3K27M-knockout cells transduced with gRNA-resistant cDNA (left) and summary data of H3K27 trimethylation normalized to total H3 (right) (*N* = 3) **(C)** Representative IF images of SU-DIPG-XVII cells stained for H3K27me3 (green), EdU (magenta), and DAPI (blue); Left panels: parental cells; middle panels: cells transduced with control sgRNA

lentivirus; right panels: cells transduced with gRNA targeting *H3-3A*; **(D)** Quantification of EdU-positive cells in (C) (*N* = 3) **(E)** Cell-viability assays at each time point were performed (*N* = 3), with 3 wells per condition (*n* = 3) ; **(F)** Effect of H3.3K27M knockout in patient cells on soft-agar colony formation; **(G)** Summary data of number of colonies in (F) (*n* = 3); **(H)** H3.3K27M DIPG cells (SU-DIPG-XIII) and cells with both *H3-3A* alleles knocked out were implanted in the brain of immunocompromised mice. Tumor growth was monitored by in vivo luciferase-activity imaging. Equal numbers of cells for each condition were implanted at postnatal day 2 (P2), and representative images at P38 are shown; **(I)** Kaplan–Meier estimates of overall survival upon knockout of H3.3K27M (*P* = 0.039, SU-DIPG-XIII *n* = 5; sgRNA *H3-3A* DIPG-XIII *n* = 5); **(J)** Representative IHC images of parental (left) and knockout (right) cells stained for H3K27me3, NeuN, or GFAP (green), and Ki67 (red) and DAPI (blue) (Top row, low magnification; scale bar, 200 μm; middle and bottom rows, high magnification; scale bar, 20 μm). For immunoblotting, Edu and IF, the measurements for each experimental group/treatment were analyzed by ANOVA, followed by pairwise comparisons using two-sample t-tests. For cell viability, a linear mixed-effects model was used for the comparison. Data are presented as means $\pm$ SEM. ***$P < 0.001$; **$P < 0.01$. Probability of survival was compared using log-rank survival estimate.

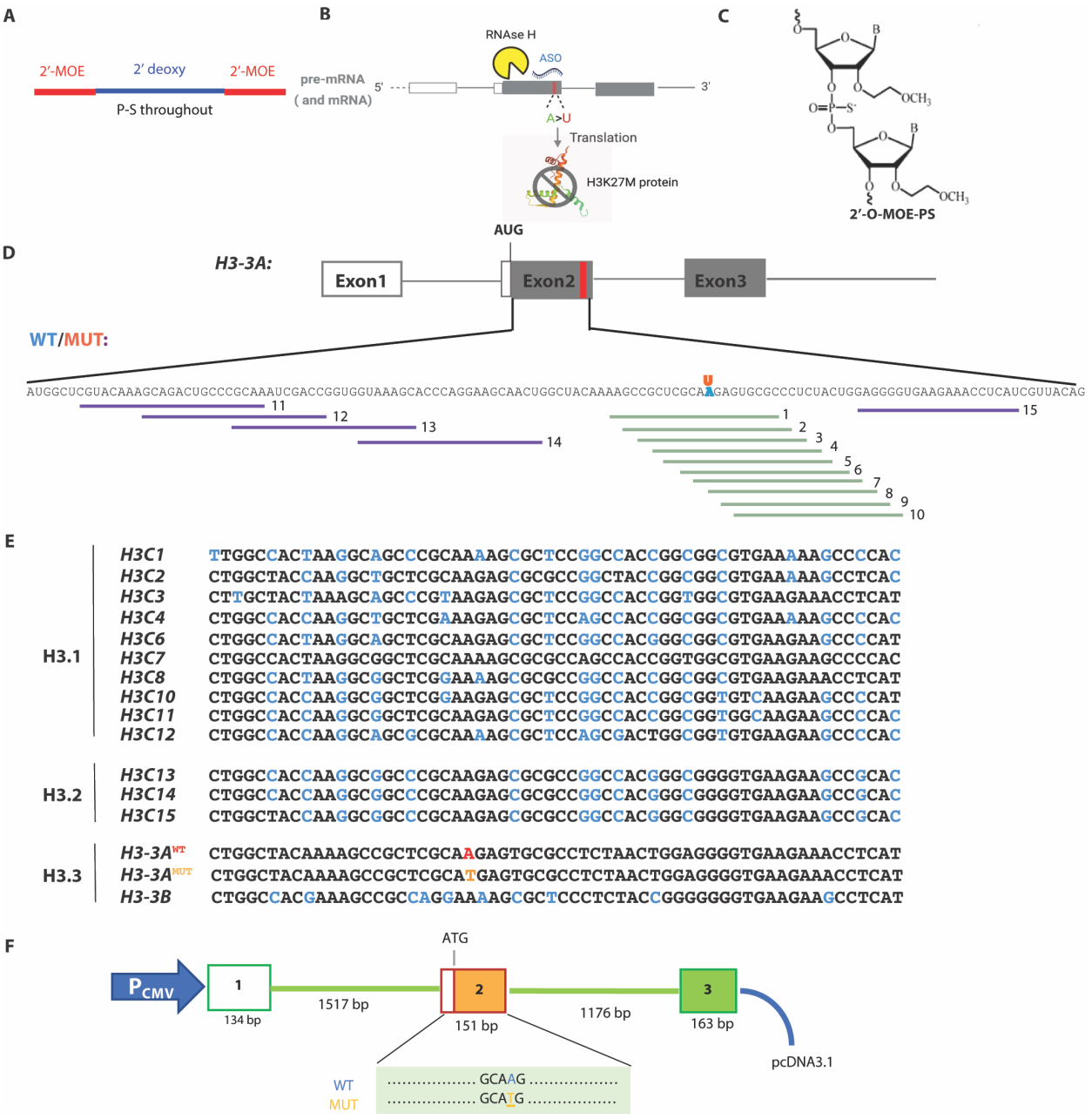

Fig. S2. Schematic representation of tested chemically modified "gapmer" ASOs targeting *H3-3A* exon 2. (**A**) Diagram of a single-stranded "gapmer" ASO with a central DNA region (blue), 2'-O-methoxyethyl (MOE) wings (red) and phosphorothioate (PS) backbones; **(B**) Mechanism of RNA knockdown by gapmer ASOs, depicting RNase-H-mediated cleavage of the RNA in DNA-RNA hybrids; (**C**) ASO chemical modifications; **(D)** The 151-nucleotide exon 2 was targeted by overlapping 20-mer ASOs at various intervals, with the position of allele-specific ASOs shown in

green and that of gene-specific ASOs shown in purple; **(E)** Sequence alignment around the mutation region, showing the *H3-3A*^{K27M} allele with T (orange) and the *H3-3A*^{WT} allele with A (red); divergent nucleotides relative to the *H3-3A*^{K27M} allele are shown in blue; **(F)** Schematic representation of the WT and MUT minigene constructs, comprising exons 1 to 3 and the intact introns.

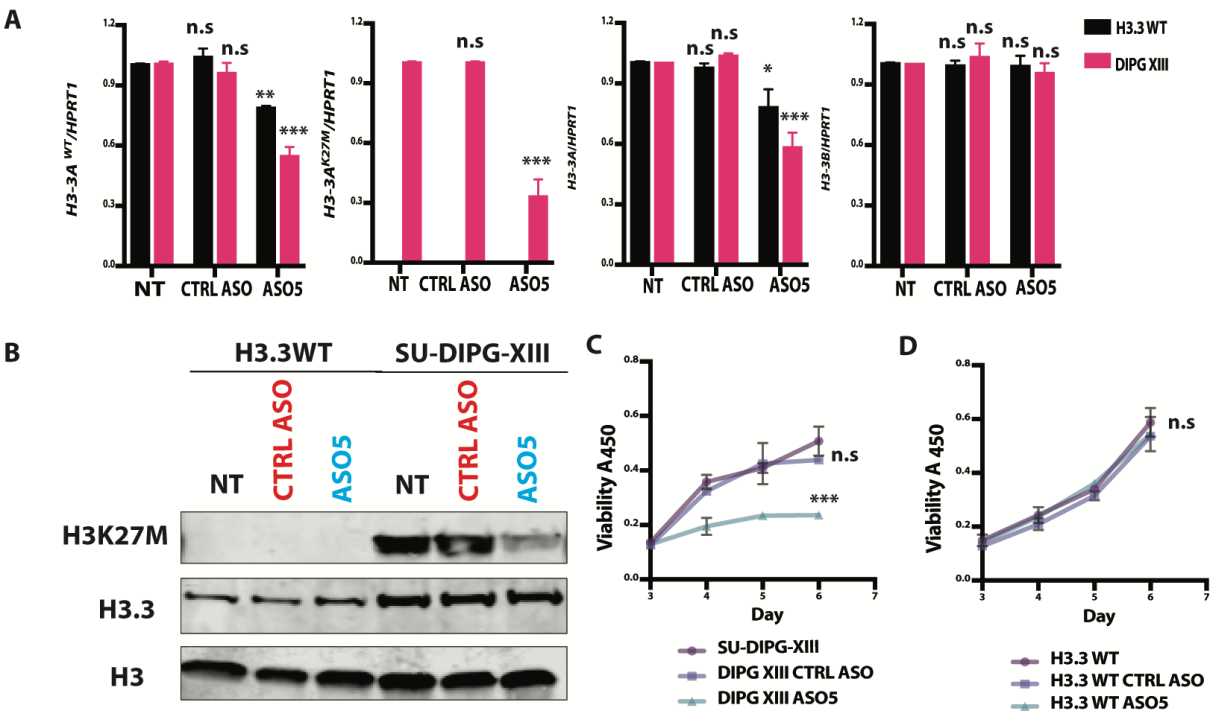

Fig. S3. Lipofectamine transfection of ASO5 into H3.3WT glioma cells and SU-DIPG-XIII cells. (A) RNA extracted from H3.3WT glioma cells (black) and SU-DIPG-XIII cells (pink), untreated or treated with CTRL ASO or ASO5, was quantified by RT-qPCR (n = 3) with gene-specific primers (right two graphs) or allele-specific primers (left two graphs) (N = 3); **(B)** Protein was detected by western blotting using H3.3K27M, H3.3, and total H3 antibodies; **(C)** Cell-viability assays at each time point for the H3.3K27M cell line (N = 3); **(D)** Same as (C) for the H3.3WT cell line. For RT-qPCR, the measurements for each experimental group/treatment were analyzed by ANOVA, followed by pairwise comparisons using two-sample t-tests. For cell viability, a linear mixed-effects model was used for the comparison. ***P < 0.001; **P < 0.01; *P < 0.05. Data are presented as means $\pm$ SEM.

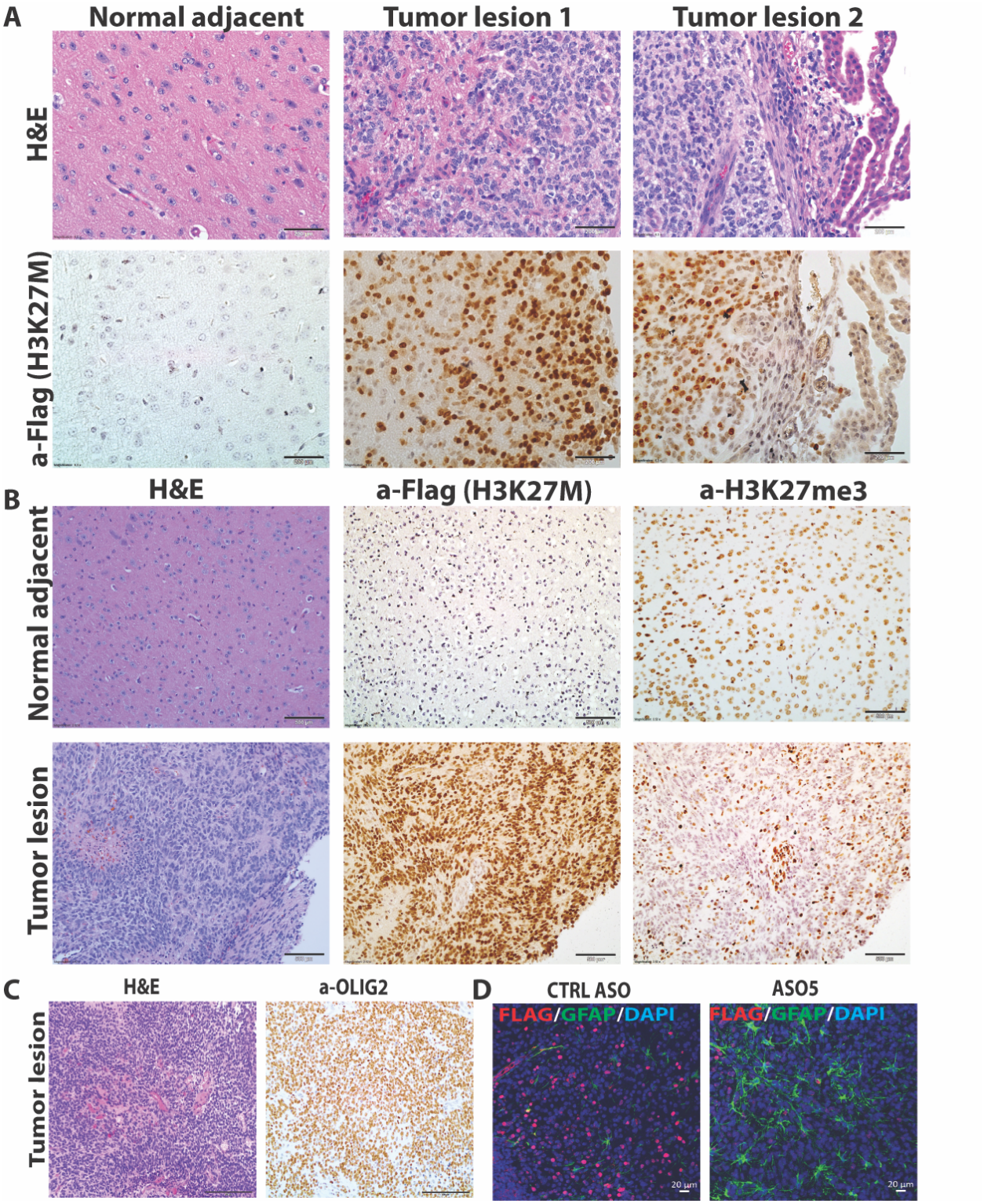
A
Normal adjacent
Tumor lesion 1
Tumor lesion 2
H&E
a-Flag (H3K27M)
B
H&E
a-Flag (H3K27M)
a-H3K27me3
Normal adjacent
Tumor lesion
C
H&E
a-OLIG2
Tumor lesion
D
CTRL ASO
ASO5
FLAG/GFAP/DAPI
FLAG/GFAP/DAPI
20 µm
20 µm

Fig. S4. RCAS-Tva mouse model resembles patient histology. (A) Representative H&E-stained sections (top row) of murine normal-adjacent (left) and tumor (middle and right) tissues, and IHC staining of Flag-tagged H3.3K27M (bottom row) (scale bar, 200 μm); **(B)** Representative H&E-stained sections (left) of murine tumors, and IHC staining with Flag (middle) and H3K27me3 (right) antibodies (scale bar, 500 μm); top row: normal adjacent tissue section; bottom row: H3.3K27M tumor section **(C)** Representative H&E-stained section ((left) and IHC staining with OLIG2 antibody (right) of murine tumor section (scale bar, 200 μm); **(D)** Representative IF co-stained Flag-tag (H3K27M, red) and GFAP (green) (Scale bar, 20 μm) in RCAS-Tva mouse model.

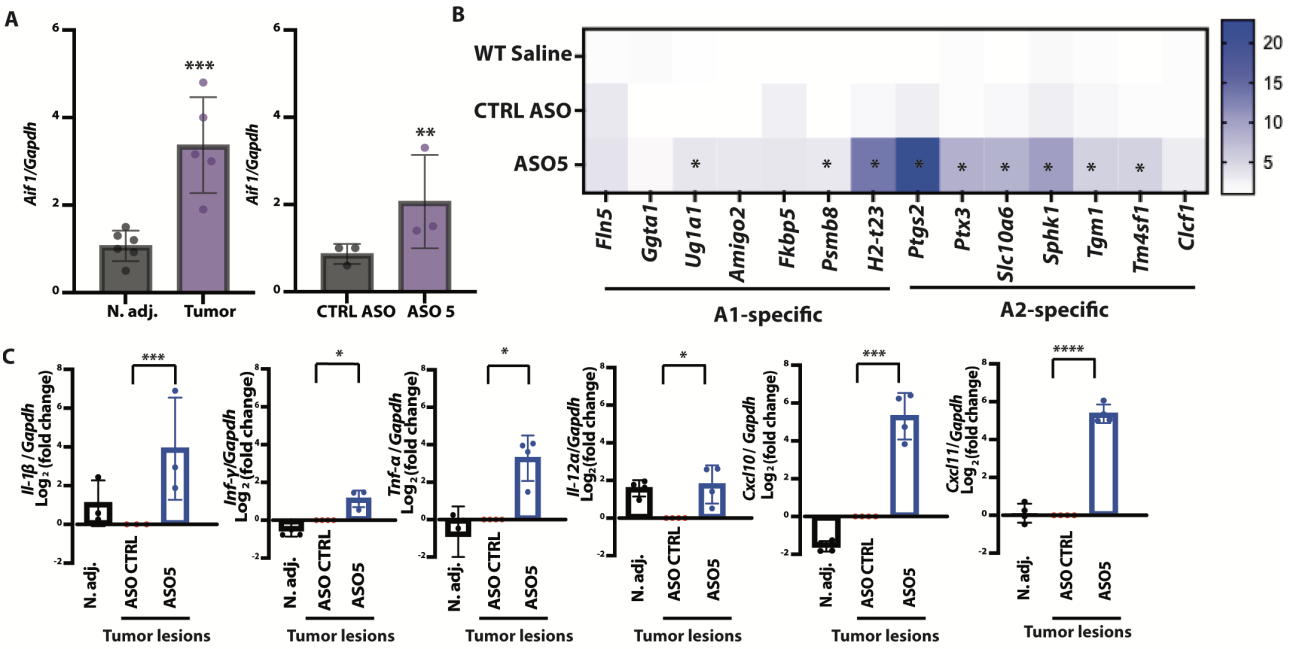

Fig. S5. ASO-mediated H3.3K27M depletion in the RCAS-Tva mouse model induced microglia activation, upregulated anti-tumor cytokines, and promoted A2-specific reactive-astrocyte differentiation. (A) Quantification of microglia-activation marker *Aif1* mRNA by RT-qPCR (n = 3), comparing normal tissue to tumor lesions (left) and CTRL ASO versus ASO5 treatment in tumor lesions (right) ($N \geq 3$). **(B)** Heat map of A1- and A2-specific astrocyte markers, measured by RT-qPCR (n = 3), in uninfected saline-treated mice (top), and CTRL ASO-treated (middle) or ASO5-treated (bottom) H3.3K27M mice (N=5); **(C)** Summary data of mRNA expression, measured by RT-qPCR (n = 3), of anti-tumor cytotoxic factors: Il-1β, Tnf-α, Inf-γ, Il-12$^{\alpha}$, Cxcl10, and Cxcl11 in untreated normal-adjacent tissues, and in tumor-lesion tissues from mice treated with CTRL ASO or ASO5 (N= 4). For RT-qPCR experiments, Welch's two-sample t-test was used to compare two groups. ****$P < 0.0001$; ***$P < 0.001$; **$P < 0.01$; *$P < 0.05$. Data are presented as means $\pm$ SEM.

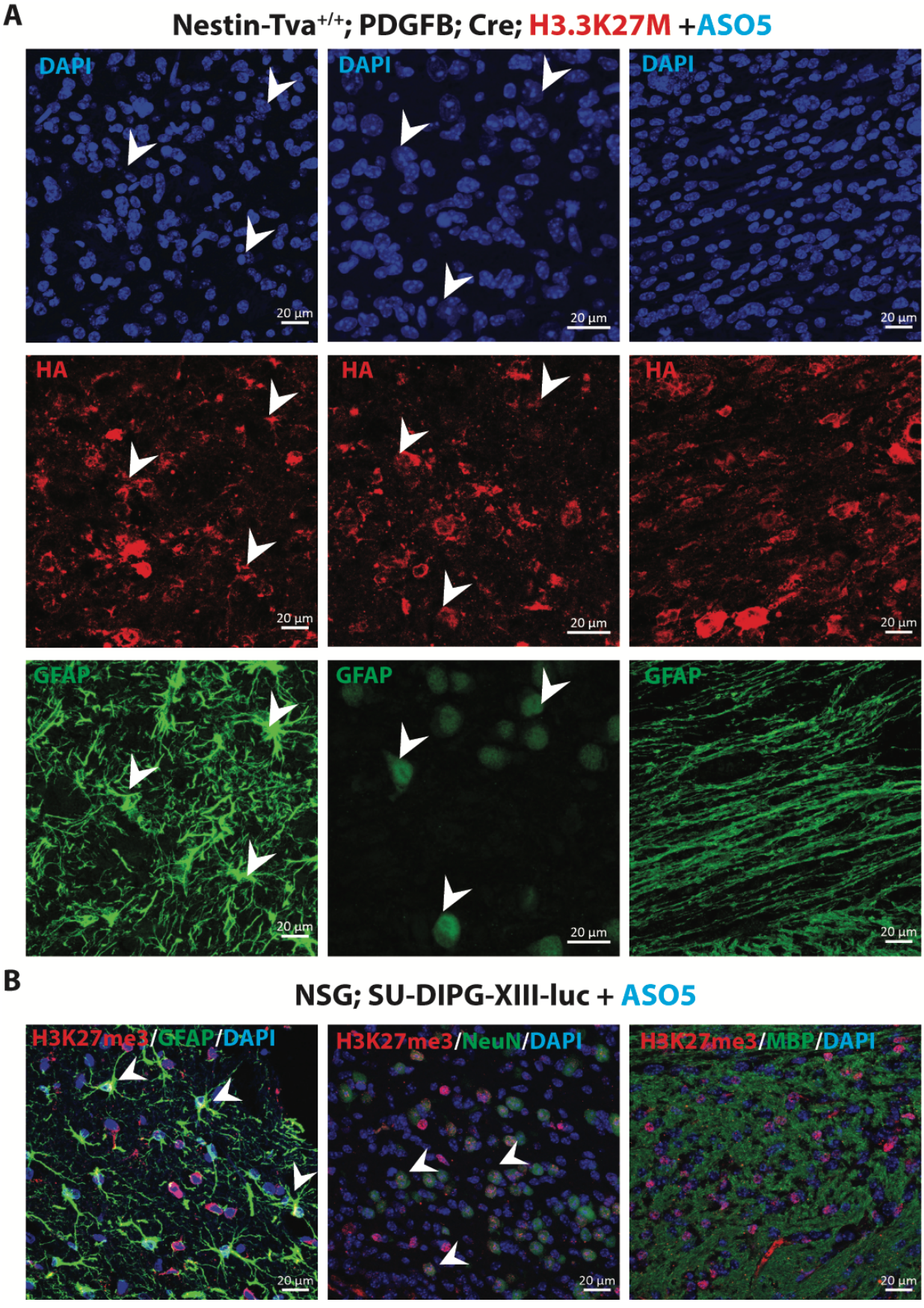
A
Nestin-Tva+/+; PDGFB; Cre; H3.3K27M +ASO5
DAPI
HA
GFAP
20 µm
B
NSG; SU-DIPG-XIII-luc + ASO5
H3K27me3/GFAP/DAPI
H3K27me3/NeuN/DAPI
H3K27me3/MBP/DAPI

Fig. S6. ASO5 treatment promoted differentiation of tumor cells in both mouse models. (A) RCAS-Tva mouse model tumor sections were stained with HA-tag antibody (red, for tagged PDGFB and Cre) and DAPI (blue) plus either GFAP, NeuN, or MBP antibodies (green). Representative image with single channels of DAPI (top), HA (middle), and GFAP (bottom left), NeuN (bottom middle) or MBP (bottom right) (*N* = 5); **(B**) Representative IF images of tumor sections co-stained with H3K27me3 (red) and (in green) GFAP (left), NeuN (middle) or MBP (right) in the SU-DIPG-XIII-*Luc* orthotopic xenograft mouse model (*N* = 5). Arrowheads in both panels indicate co-localization of either HA tag (A) or H3K27me3 (B) with differentiation markers. Scale bar, 20 μm.

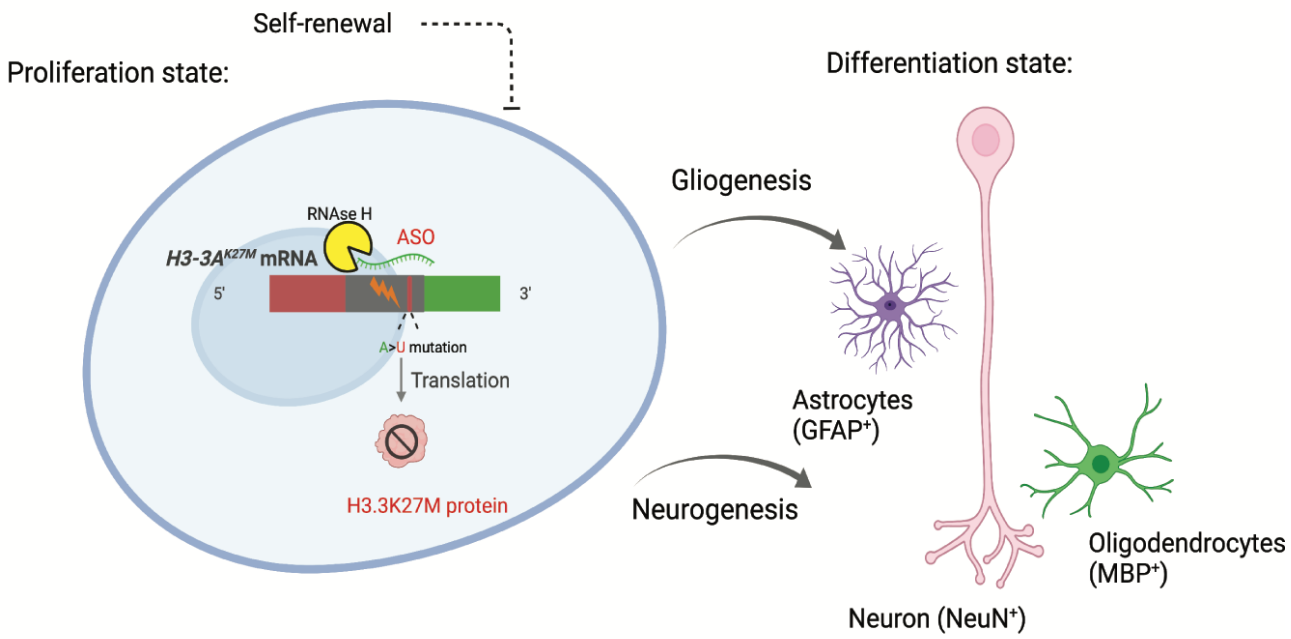

Fig. S7. Schematic model of ASO treatment in H3.3K27M DIPG mouse models. The H3.3K27M oncoprotein blocks cell differentiation, such that the neural stem cells continue to proliferate. ASO5-mediated H3.3K27M depletion inhibits their proliferation, and promotes tumor-cell neurogenesis into NeuN$^+$ neurons, and gliogenesis into GFAP$^+$ astrocytes and MBP$^+$ oligodendrocytes.

Supplemental Table S1:

List of ASOs	
CTRL ASO	CCTTCCCTGAAGGTTCCTCC
ASO1	CACTCATGCGAGCGGCTTTT
ASO2	GCACTCATGCGAGCGGCTTT
ASO3	CGCACTCATGCGAGCGGCTT
ASO4	GCGCACTCATGCGAGCGGCT
ASO5	GGCGCACTCATGCGAGCGGC
ASO6	GGGCGCACTCATGCGAGCGG
ASO7	AGGGCGCACTCATGCGAGCG
ASO8	GAGGGCGCACTCATGCGAGC
ASO9	AGAGGGCGCACTCATGCGAG
ASO10	TAGAGGGCGCACTCATGCGA
ASO11	GGGCAGTCTGCTTTGTACGA
ASO12	CGATT TGCGGGCAGTCTACT
AS013	TACCACCGGTCGATTTGCGG
AS014	TTGCTTCCTGGGTGCTTTAC
AS015	GAGGT TTCTTCACCCCTCCA

Supplemental Table S2:

Primers for gDNA *H3-3A*	Fwd5'-GGATCCGGCGGCGTGTGTTGGGGGATAGCCT
	Rev5'CTTGAATTCTCACTGCAAAGCACCGATAGCTGC
Primers for *H3-3B*:	Fwd 5'- GTGCTGGTTTTTCGCTCGTC
	Rev 5'- CTTTCGTGGCCAGCTGTTTG
Primers for *H3-3A*:	Fwd 5'- GGACTTTAAAACAGATCTGCGCTT
	Rev 5'- GTCTTTTGGCATAATTGTTACACGT
Primers for *HPRT1*:	Fwd 5'- TGACCAGTCAACAGGGGACA
	Rev 5'- TGCCTGACCAAGGAAAGCAA
Primers for *H3-3A*^{K27M}:	Fwd 5'- GCTACAAAAGCCGCTCGAAT
	Rev 5'- CCAGACGCTGGAAGGGAAGT
Primers for *H3-3A* ^{K27M} in minigene:	Fwd 5'- GCTACAAAAGCCGCTCGAAT
	Rev 5'-ATCTGCAGAATTCTCACTGC
Primers for *H3-3A*^{WT}	Fwd 5'- GCTACAAAAGCCGCTCTCAA
	Rev 5'- CCAGACGCTGGAAGGGAAGT
Primers for *H3-3A*^{WT} in minigene:	Fwd 5'- GCTACAAAAGCCGCTCTCAA
	Rev 5'-ATCTGCAGAATTCTCACTGC